Crystal structure of BaMn$_2$(AsO$_4$)$_2$ containing discrete [Mn$_4$O$_{18}$]$^{28-}$ units

Salvador Alcantar, Hollis R. Ledbetter and Kulugammana G. S. Ranmohotti*

Division of Science, Mathematics and Technology, Governors State University, 1 University Parkway, University Park, IL 60484-0975, USA. *Correspondence e-mail: kranmohotti@govst.edu

In our attempt to search for mixed alkaline-earth and transition metal arsenates, the title compound, barium dimanganese(II) bis(arsenate), has been synthesized by employing a high-temperature RbCl flux. The crystal structure of BaMn$_2$(AsO$_4$)$_2$ is made up of MnO$_6$ octahedra and AsO$_4$ tetrahedra assembled by sharing corners and edges into infinite slabs with composition [Mn$_2$(AsO$_4$)$_2$]$^{2-}$ that extend parallel to the *ab* plane. The barium cations reside between parallel slabs maintaining the interslab connectivity through coordination to eight oxygen anions. The layered anionic framework comprises weakly interacting [Mn$_4$O$_{18}$]$^{28-}$ tetrameric units. In each tetramer, the manganese(II) cations are in a planar arrangement related by a center of inversion. Within the slabs, the tetrameric units are separated from each other by 6.614 (2) Å (Mn···Mn distances). The title compound has isostructural analogues amongst synthetic SrM_2(XO$_4$)$_2$ compounds with M = Ni, Co, and X = As, P.

1. Chemical context

Compounds of vanadates, phosphates, and arsenates with the general formula $AM_2(XO_4)_2$, where A = Pb or an alkaline earth metal, M = Mg or a divalent first row transition metal, and X = V, P or As, can adopt different structure types. They have attracted much attention in solid-state physics due to magnetic ordering at low temperatures and the occurrence of (multiple) phase transitions. For $AM_2(XO_4)_2$ compounds with Pb or an alkaline earth metal ion on the A^{2+} site and a transition metal with partially filled 3d orbitals on the M^{2+} site, one-dimensional magnetic properties with high anisotropy and weak interchain interactions have been reported (Bera *et al.*, 2013). The crystal structures of some of these compounds comprise screw-chains made up of MO$_6$ octahedra, separated by non-magnetic VO$_4$ (V^{5+}; 3d^0) tetrahedra, resulting in a quasi one-dimensional structure. Five representatives of this family have been characterized crystallographically, *viz.* BaMg$_2$(VO$_4$)$_2$ (Velikodnyi *et al.*, 1982), BaCo$_2$(VO$_4$)$_2$ (Wichmann & Müller-Buschbaum, 1986*a*), BaMn$_2$(VO$_4$)$_2$, BaMgZn(VO$_4$)$_2$ and Ba$_{1/2}$Sr$_{1/2}$Ni$_2$(VO$_4$)$_2$ (Von Postel & Müller-Buschbaum, 1992). They crystallize in the tetragonal crystal system in space group $I4_1/acd$ (No. 142). For the related compounds SrMn$_2$(VO$_4$)$_2$ (Niesen *et al.*, 2011), SrCo$_2$(VO$_4$)$_2$ (Osterloh & Müller-Buschbaum, 1994*a*), PbCo$_2$(VO$_4$)$_2$ (He *et al.*, 2007) and PbNi$_2$(VO$_4$)$_2$ (Uchiyama *et al.*, 1999), it was found that they adopt the SrNi$_2$(VO$_4$)$_2$ structure type (Wichmann & Müller-Buschbaum, 1986*b*), crystallizing in space group $I4_1cd$ (No.110), a subgroup of the latter. The only copper(II) vanadate compound with an $AM_2(XO_4)_2$ composition is BaCu$_2$(VO$_4$)$_2$ (Vogt & Müller-Buschbaum, 1990). The

0.15 mm

OPEN ACCESS

1855
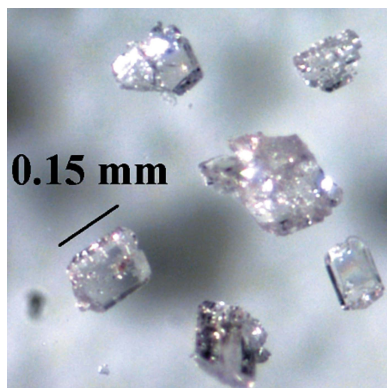
crystal structure is also tetragonal but belongs to space group $I\bar{4}2d$ (No. 122), another subgroup of $I4_1/acd$. BaNi$_2$(VO$_4$)$_2$ (Rogado et al., 2002) adopts a different structure type as it belongs to the rhombohedral space group $R\bar{3}$ (No. 148) and represents the only quasi-two-dimensional system within the above-mentioned vanadates.

Phosphates containing transition metals have been widely investigated because of their variety of potential applications. They can adopt a plethora of different structure types and show various magnetic properties. With respect to the $AM_2(XO_4)_2$ family of compounds, the phosphates BaCu$_2$(PO$_4$)$_2$ (Moqine et al., 1993), α-SrCo$_2$(PO$_4$)$_2$ (El Bali et al., 1993a), β-SrCo$_2$(PO$_4$)$_2$ (Yang et al., 2016), SrNi$_2$(PO$_4$)$_2$ (El Bali et al., 1993b), SrNiZn(PO$_4$)$_2$ (El Bali et al., 2004) and SrMn$_2$(PO$_4$)$_2$ (El Bali et al., 2000) crystallize in space group $P\bar{1}$ (No. 2). SrCu$_2$(PO$_4$)$_2$ (Belik et al., 2005) and PbCu$_2$(PO$_4$)$_2$ (Belik et al., 2006) are isotypic and crystallize in the ortho-rhombic crystal system [space group $Pccn$ (No. 56)]. The crystal structures of BaNi$_2$(PO$_4$)$_2$ (Čabrić et al., 1982), and BaFe$_2$(PO$_4$)$_2$ (Kabbour et al., 2012) possess trigonal symmetry in space group $R\bar{3}$ (No. 148). BaCo$_2$(PO$_4$)$_2$, in particular, can exist in several polymorphs such as the rhombohedral γ-phase [($R\bar{3}$ (No. 148); Bircsak & Harrison, 1998], the monoclinic α-phase [$P2_1/a$ (No. 14)] and the trigonal β-phase [$P\bar{3}$ (No. 147); David et al., 2013], depending on the synthetic conditions and thermal history. It has been reported that α-SrZn$_2$(PO$_4$)$_2$ (Hemon & Courbion, 1990) and SrFe$_2$(PO$_4$)$_2$ (Belik et al., 2001) adopt different structure types and crystallize in the monoclinic space group $P2_1/c$ (No. 14).

Thus far, compared to vanadates and phosphates, only a few arsenates of the $AM_2(XO_4)_2$ family have been studied, viz. BaNi$_2$(AsO$_4$)$_2$ (Eymond et al., 1969a), BaMg$_2$(AsO$_4$)$_2$ and BaCo$_2$(AsO$_4$)$_2$ (Eymond et al., 1969b) in space group $R\bar{3}$, and SrCo$_2$(AsO$_4$)$_2$ (Osterloh & Müller-Buschbaum, 1994a) and BaCu$_2$(AsO$_4$)$_2$ (Osterloh & Müller-Buschbaum, 1994b) in space groups $P\bar{1}$ and $P2_1/n$, respectively. To extend our knowledge of the $AM_2(XO_4)_2$ system, we have undertaken an investigation of the BaO/MnO/As$_2$O$_5$ phase diagram and employed a flux method for crystal growth. The present work deals with the determination of the crystal structure of a new mixed-metal orthoarsenate, BaMn$_2$(AsO$_4$)$_2$.

2. Structural commentary

Besides Ba$_2$Mn(AsO$_4$)$_2$ (Adams et al., 1996), BaMn$_2$(AsO$_4$)$_2$ represents the second compound to be structurally characterized in the system BaO/MnO/As$_2$O$_5$. BaMn$_2$(AsO$_4$)$_2$ is isotypic with β-SrCo$_2$(PO$_4$)$_2$ (Yang et al., 2016), SrCo$_2$(AsO$_4$)$_2$ (Osterloh & Müller-Buschbaum, 1994a) and SrNi$_2$(PO$_4$)$_2$ (El Bali et al., 1993b) (for numerical data for these structures, see
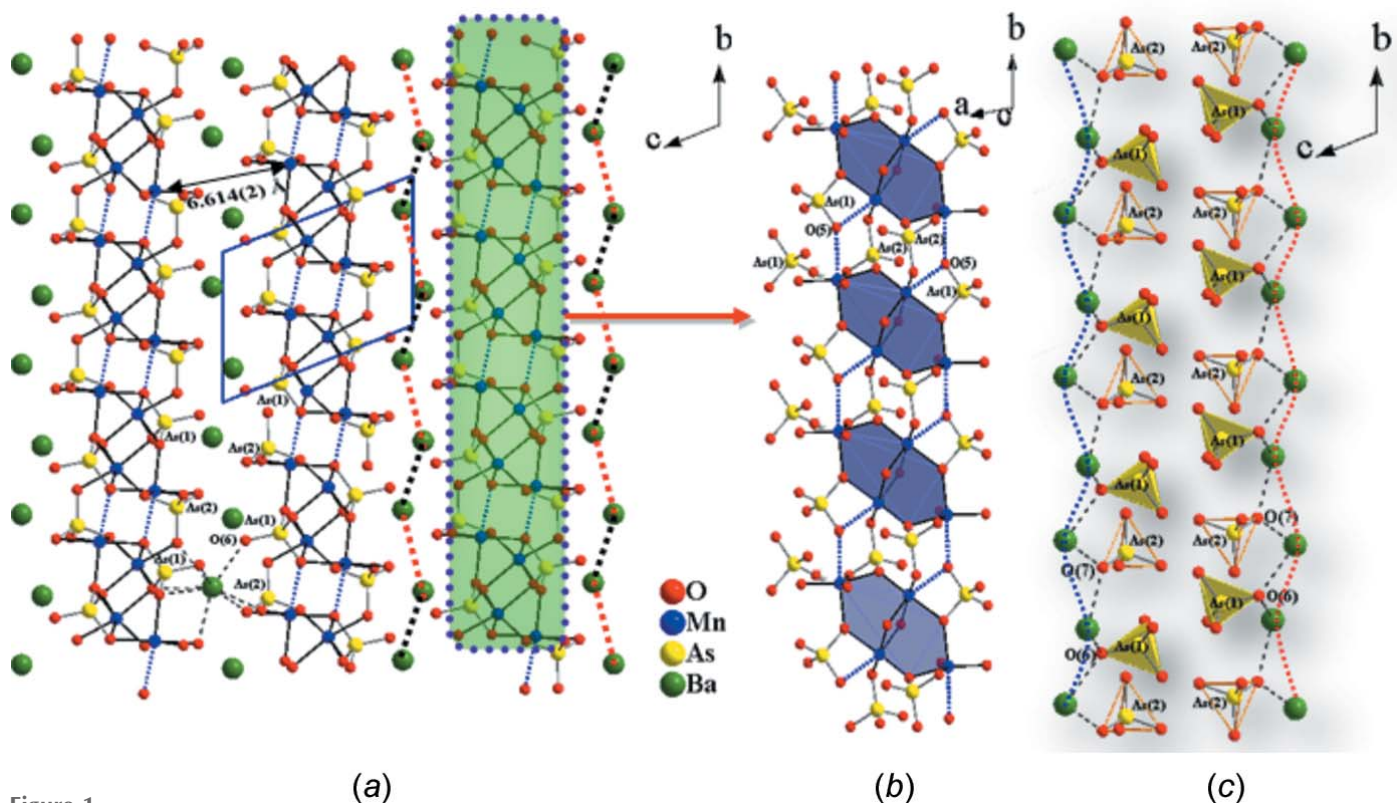
Figure 1
(a) Perspective view of the crystal structure of BaMn$_2$(AsO$_4$)$_2$ viewed along the a axis. The quasi-two-dimensional lattice is characterized by [Mn$_2$(AsO$_4$)$_2$]$^{2-}$ slabs, which are highlighted by dark- and light-colored lines representing the Mn—O and As—O bonds, respectively. The wavy and dotted lines (right) indicate the zigzag arrays of barium cations. Only one barium cation with bonds is drawn for clarity, demonstrating the function of Ba—O bonds with regard to holding neighboring [Mn$_2$(AsO$_4$)$_2$]$^{2-}$ slabs. (b) Part of the crystal structure showing corner- and edge-sharing MnO$_6$ octahedra and AsO$_4$ tetrahedra. In each tetramer, the manganese(II) atoms are in a planar configuration related by a center of inversion. (c) Polyhedral representation showing the alternating arrangement of isolated arsenate units. Only two bonds (dotted lines) around barium are shown for clarity.
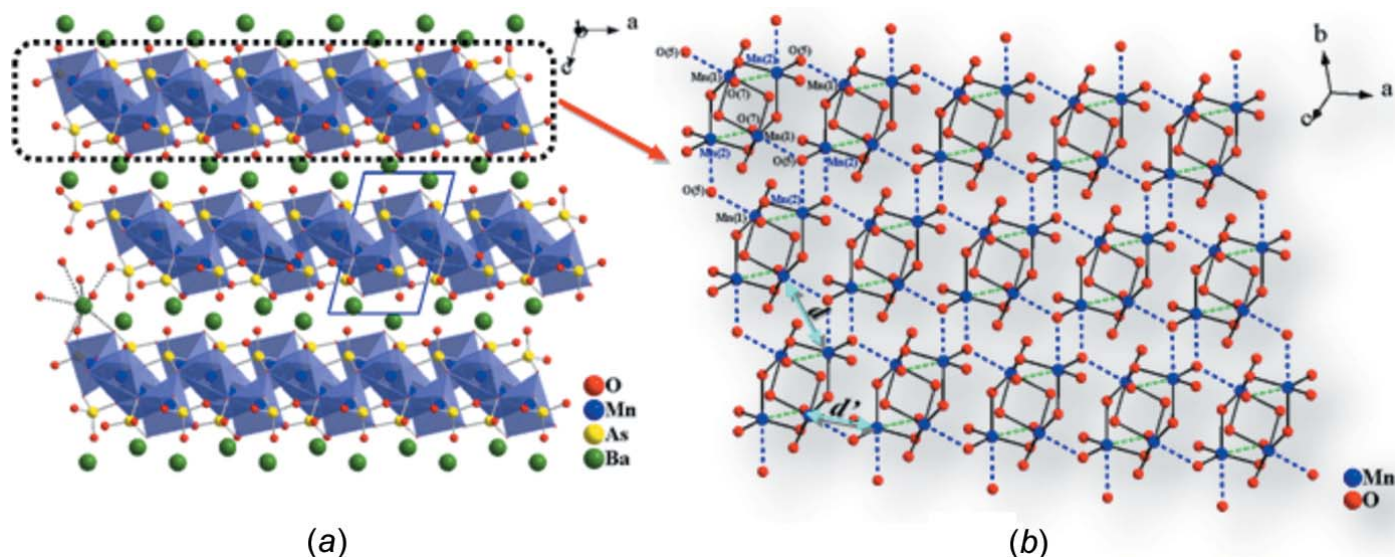
Figure 2
(*a*) Quasi-two-dimensional structure of $BaMn_2(AsO_4)_2$ shown by polyhedral and ball-and-stick drawing viewed along the *b* axis. (*b*) Ball-and-stick drawing of a portion of the manganese oxide network formed by interconnected tetrameric units. Dashed lines represent long Mn—O bonds.

Supplementary Table 1 in the *Supporting information*). The crystal structure of $BaMn_2(AsO_4)_2$ can be described as a three-dimensional framework containing slabs of composition $[Mn_2(AsO_4)_2]^{2-}$ that are built up from two different MnO_6 and two different AsO_4 polyhedra (Fig. 1) and extend parallel to the *ab* plane (Fig. 2). Mn1 possesses a distorted octahedral coordination environment and exhibits five normal Mn—O bonds and one long Mn—O bond. Mn2 is also six-coordinated and has two long Mn—O bonds, again forming a distorted MnO_6 octahedron (Table1, Fig. 3*a*). Similar distortions in MnO_6 octahedra have been observed previously (Adams *et al.*, 1996; Weil & Kremer, 2017). The two arsenic atoms are part of AsO_4 tetrahedra (Fig. 3*b*), with As—O bond lengths ranging from 1.663 (5)–1.710 (4) Å (Table 1) and O—As—O bond angles from 99.8 (2)–114.6 (2)°. The average As—O bond length (1.688 Å) in the title compound is identical to those of previously reported arsenates (Ulutagay-Kartin *et al.*, 2003). The bond lengths are also consistent with the sum of the Shannon crystal radii (Shannon, 1976), 1.68 Å, of four-coordinate As^{5+} (0.475 Å) and two-coordinate O^{2-} (1.21 Å). The

barium cations reside between parallel slabs and maintain the interslab connectivity through coordination to eight oxygen anions (Fig. 3*c*). The average Ba—O bond length, 2.83 Å, matches closely with 2.77 Å, the sum of the Shannon radii for eight-coordinate Ba^{2+} (1.56 Å) and two-coordinated O^{2-} (1.21 Å) ions, and is in agreement with those of other barium arsenates (Weil, 2016).

Fig. 4*a* shows two $Mn1O_6$ octahedra sharing a common edge, $O1^v$—$O1^{vii}$ (symmetry codes refer to Table 1) to form a Mn_2O_{10} unit with an Mn1$\cdots$Mn1 separation of 3.1854 (17) Å and an Mn1—O1—Mn1 angle of 93.34 (18)°. $Mn2O_6$ octahedra share corners with the Mn_2O_{10} unit through O3 and O4, resulting in a tetrameric $[Mn_4O_{18}]^{28-}$ unit (Fig. 4*b*). These $[Mn_4O_{18}]^{28-}$ units are interlinked through AsO_4 tetrahedra to give slabs with overall composition $[Mn_2(AsO_4)_2]^{2-}$. Each $[Mn_4O_{18}]^{28-}$ unit interacts weakly by sharing oxygen vertices with six other units, whereby the tetrameric units are separated from each other along the *b* axis by 4.2616 (19) Å $[Mn1\cdots Mn2(1-x, -y, 2-z)]$ and along the *a* axis by 3.490 (18) Å $[Mn1\cdots Mn2(x, -1+y, -1+z)]$. The distance between the Mn atoms of adjacent slabs $[Mn2\cdots Mn2(-x, 1-y, -z)]$ is 6.614 (2) Å (Fig. 1*a*).
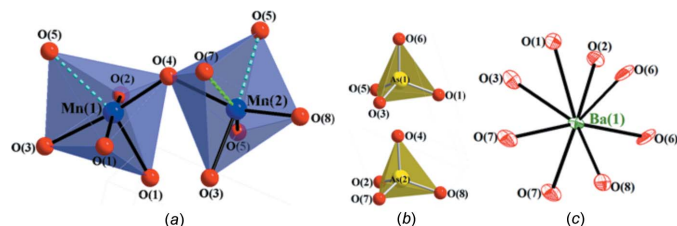

Figure 3
(*a*) Part of the crystal structure showing $Mn1O_6$ and $Mn2O_6$ octahedra sharing corners (polyhedral drawing). To distinguish the two types of bonds (short and long), one is highlighted with solid Mn—O bonds (short) and the other in dotted bonds (long). (*b*) The polyhedral units represent arsenic-centered oxygen tetrahedra. (*c*) The barium cation resides in a BaO_8 environment. Displacement ellipsoids represent the 95% probability level.

Table 1
Selected bond lengths (Å).

Mn1—O4^i	2.052 (5)	Mn2—O7	2.518 (5)
Mn1—O2^{ii}	2.108 (5)	Mn2—O5^{vi}	2.526 (5)
Mn1—O1^{iii}	2.179 (4)	As1—O6	1.663 (5)
Mn1—O1^{iv}	2.200 (5)	As1—O1	1.697 (5)
Mn1—O3	2.202 (5)	As1—O5	1.709 (5)
Mn1—O5	2.491 (5)	As1—O3	1.710 (4)
Mn2—O8^v	2.094 (5)	As2—O7	1.669 (5)
Mn2—O4	2.136 (5)	As2—O2	1.677 (5)
Mn2—O5^{iv}	2.152 (5)	As2—O8	1.677 (4)
Mn2—O3	2.178 (5)	As2—O4	1.698 (5)

Symmetry codes: (i) $-x+1, -y+2, -z+1$; (ii) $x, y+1, z$; (iii) $x+1, y, z$; (iv) $-x, -y+2, -z+1$; (v) $x-1, y, z$; (vi) $x, y-1, z$.
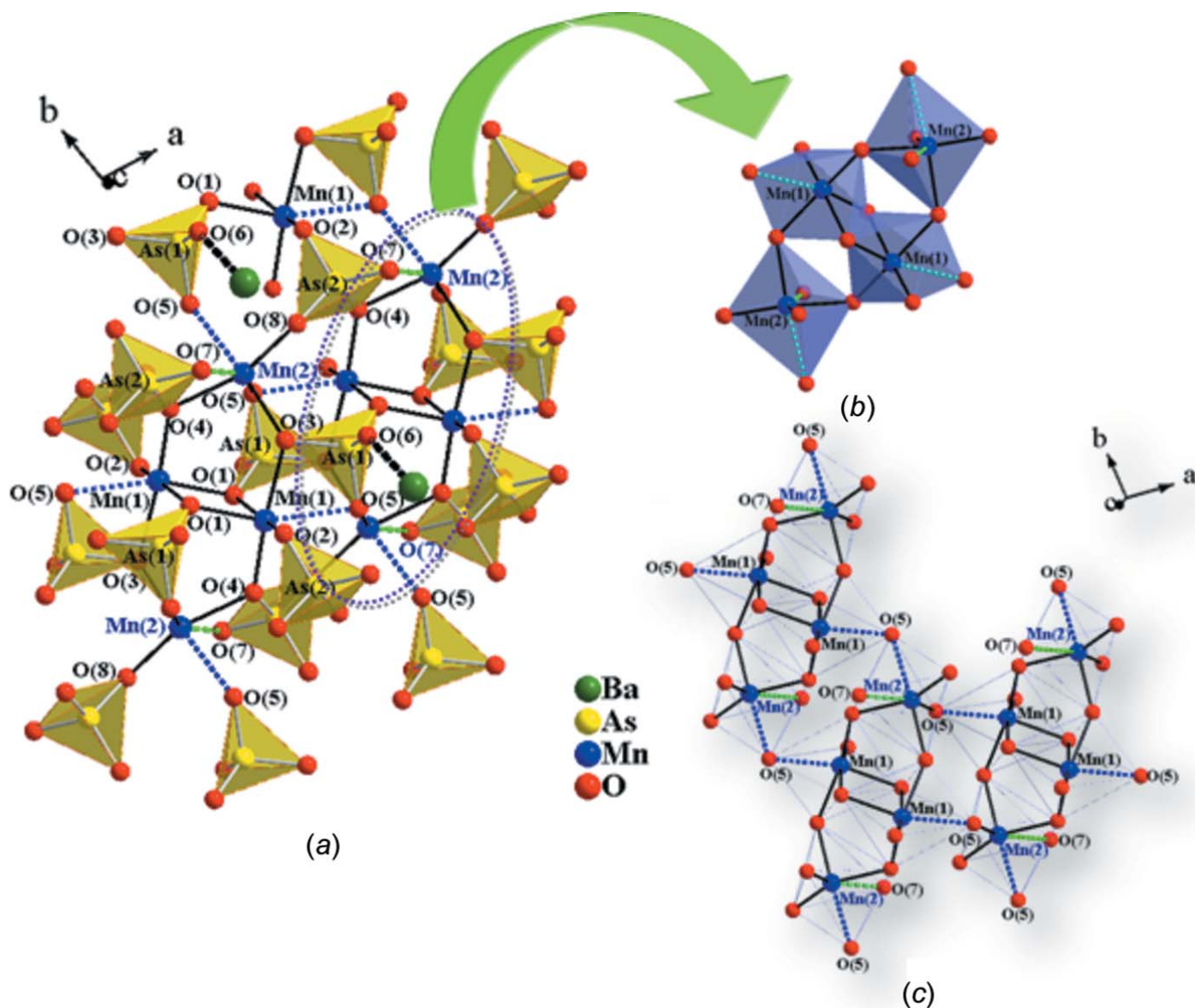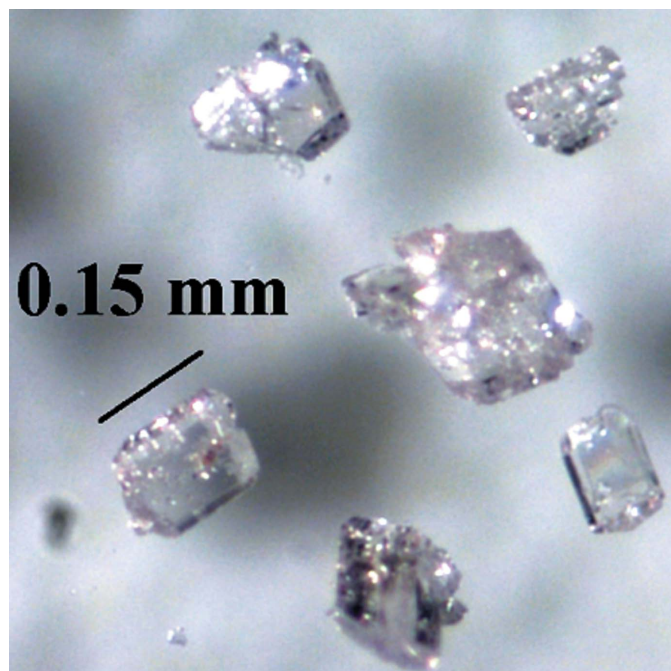
Figure 4
(a) The ball-and-stick and polyhedral composite representation showing parts of the Mn—As—O framework. The polyhedral units represent AsO_4 tetrahedra. One of the $[Mn_4O_{18}]^{28-}$ units is located in the area outlined by a dotted ellipsoid. The only unshared oxygen atom, O6 of the $As1O_4$ tetrahedra, forms a bond with a Ba cation. (b) A tetrameric unit formed by two edge-sharing $Mn1O_6$ octahedra and two corner-sharing $Mn2O_6$ octahedra. (c) Three $[Mn_4O_{18}]^{28-}$ units showing the intertetramer interaction through long Mn1—O5 and Mn2—O5 bonds (dotted lines).

As shown in Fig. 4a, the roles of the two arsenate groups are different. $As1O_4$ tetrahedra share oxygen atoms O1 with $Mn1O_6$ octahedra, and O3 and O5 atoms with $Mn1O_6$ and $Mn2O_6$ octahedra while oxygen atom O6 points towards neighboring slabs to form a bond with a Ba^{2+} cation (Fig. 4a). $As2O_4$ tetrahedra, on the other hand, share an edge (O4–O7) with $Mn2O_6$ octahedra of one tetrameric unit and share two corners (O7 and O8) with $Mn1O_6$ and $Mn2O_6$ octahedra of two other neighboring tetrameric units. Thus $As1O_4$ and $As2O_4$ tetrahedra interlink two and three neighboring tetrameric units, respectively. As shown in Fig. 1c, $As1O_4$ and $As2O_4$ tetrahedra alternate along the b axis, and this template-like arrangement allows the barium cations to propagate in a zigzag fashion to maintain the distance between the $[Mn_2(AsO_4)_2]^{2-}$ slabs.

Bond-valence sum (BVS) calculations (Brese & O'Keefe, 1991) for $BaMn_2(AsO_4)_2$ result in values of 2.19, 1.84, 4.87, 5.05 and 1.98 valence units for Mn1, Mn2, As1, As2 and Ba1, respectively, which in each case is close to the expected values of 2 for Mn, 5 for As and 2 for Ba.

It is important to note that the barium cations reside in the gaps between adjacent $[Mn_2(AsO_4)_2]^{2-}$ slabs. The large inter-slab separation [6.614 (2) Å] leads us to believe that magnetic interactions that occur between these slabs are expected to be extremely weak, and the dominant magnetic exchange is expected to appear between Mn^{2+} ions in the tetrameric units within a slab. Judging from the reported magnetic properties for related $BaM_2(XO_4)_2$ (M = Co, Ni; X = As, P) compounds with the magnetic ions sitting on a honeycomb lattice (Martin et al., 2012), or those of β-$SrCo_2(PO_4)_2$ (Yang et al., 2016) and

Figure 5
Single crystals of $BaMn_2(AsO_4)_2$ obtained from a RbCl flux.

SrNi$_2$(PO$_4$)$_2$ (He *et al.*, 2008), we also expect interesting magnetic phenomena for $BaMn_2(AsO_4)_2$.

3. Synthesis and crystallization

Light-pink crystals of $BaMn_2(AsO_4)_2$ were grown by employing an RbCl flux in a fused silica ampoule under vacuum. MnO (3.81 mmol, 99.999+%, Alfa), BaO (1.90 mmol, 99.99+%, Aldrich) and As$_2$O$_5$ (1.90 mmol, 99.9+%, Strem) were mixed and ground with RbCl (1:3 by weight) in a nitrogen-blanketed drybox. The resulting mixture was heated to 818 K at 1 K min^{-1}, isothermed for two days, heated to 1023 K at 1 K min^{-1}, isothermed for another four days, then slowly cooled to 673 K at 0.1 K min^{-1}, followed by furnace-cooling to room temperature. Prismatic crystals of $BaMn_2(AsO_4)_2$ (Fig. 5) were retrieved upon washing off recrystallized RbCl with deionized water.

4. Refinement

Crystal data, data collection and structure refinement details are summarized in Table 2. The final Fourier difference synthesis showed the maximum residual electron density 0.96 Å from Ba1 and the minimum 0.83 Å from the same site.

Acknowledgements

Table 2
Experimental details.

Crystal data	
Chemical formula	$BaMn_2(AsO_4)_2$
M_r	525.06
Crystal system, space group	Triclinic, $P\bar{1}$
Temperature (K)	293
a, b, c (Å)	5.7981 (12), 7.0938 (14), 9.817 (2)
α, β, γ (°)	109.75 (3), 100.42 (3), 98.40 (3)
V (Å^3)	364.26 (15)
Z	2
Radiation type	Mo $K\alpha$
μ (mm^{-1})	17.78
Crystal size (mm)	$0.20 \times 0.10 \times 0.06$
Data collection	
Diffractometer	Rigaku AFC8S
Absorption correction	Multi-scan (*REQAB*; Rigaku, 1998)
T_{min}, T_{max}	0.808, 1.000
No. of measured, independent and observed [$I > 2\sigma(I)$] reflections	3149, 1330, 1254
R_{int}	0.035
$(\sin \theta/\lambda)_{max}$ (Å^{-1})	0.606
Refinement	
$R[F^2 > 2\sigma(F^2)]$, $wR(F^2)$, S	0.039, 0.097, 1.14
No. of reflections	1330
No. of parameters	119
$\Delta\rho_{max}, \Delta\rho_{min}$ (e Å^{-3})	3.25, −2.93

Computer programs: *CrystalClear* (Rigaku, 2006), *SHELXT* (Sheldrick, 2015*a*), *SHELXL2014* (Sheldrick, 2015*b*), *DIAMOND* (Brandenburg, 1999) and *publCIF* (Westrip, 2010).

References

Adams, R., Layland, R. & Payen, C. (1996). *Polyhedron*, **15**, 1235–1239.

Belik, A. A., Azuma, M., Matsuo, A., Kaji, T., Okubo, S., Ohta, H., Kindo, K. & Takano, M. (2006). *Phys. Rev. B*, **73**, 024429-1–024429-7.

Belik, A. A., Azuma, M., Matsuo, A., Whangbo, M., Koo, H. J., Kikuchi, J., Kaji, T., Okubo, S., Ohta, H., Kindo, K. & Takano, M. (2005). *Inorg. Chem.* **44**, 6632–6640.

Belik, A. A., Lazoryak, B. I., Pokholok, K. V., Terekhina, T. P., Leonidov, I. A., Mitberg, E. B., Karelina, V. V. & Kellerman, D. G. (2001). *J. Solid State Chem.* **162**, 113–121.

Bera, A. K., Lake, B., Islam, A. T. M. N., Klemke, B., Faulhaber, E. & Law, J. M. (2013). *Phys. Rev. B*, **87**, 224423-1–224423-10.

Bircsak, Z. & Harrison, W. T. A. (1998). *Acta Cryst.* C**54**, 1554–1556.

Brandenburg, K. (1999). *DIAMOND*. Crystal Impact GbR, Bonn, Germany.

Brese, N. E. & O'Keeffe, M. (1991). *Acta Cryst.* B**47**, 192–197.

Čabrić, B., Žižić, B. & Napijalo, M. L. (1982). *J. Cryst. Growth*, **60**, 169–171.

David, R., Kabbour, H., Pautrat, A. & Mentré, O. (2013). *Inorg. Chem.* **52**, 8732–8737.

El Bali, B., Boukhari, A., Aride, J. & Abraham, F. (1993*b*). *J. Solid State Chem.* **104**, 453–459.

El Bali, B., Boukhari, A., Glaum, R., Gerk, M. & Maass, K. (2000). *Z. Anorg. Allg. Chem.* **626**, 2557–2562.

El Bali, B., Boukhari, A., Holt, E. M. & Aride, J. (1993*a*). *J. Crystallogr. Spectrosc. Res.* **23**, 1001–1004.

El Bali, B., Lachkar, M., Allouchi, H. & Narymbetov, B. (2004). *Phosphorus Res. Bull.* **15**, 125–130.

Eymond, S., Martin, M. & Durif, A. (1969*a*). *C. R. Acad. Sci. Ser. C*, **286**, 1694–1696.

Eymond, S., Martin, M. & Durif, A. (1969*b*). *Mater. Res. Bull.* **4**, 595–599.

He, Z. Z., Chen, S. C., Lue, C. S., Cheng, W. D. & Ueda, Y. (2008). *Phys. Rev. B*, **78**, 212410-1–212410-4.

He, Z., Ueda, Y. & Itoh, M. (2007). *J. Solid State Chem.* **180**, 1770–1774.

Hemon, A. & Courbion, G. (1990). *J. Solid State Chem.* **85**, 164–168.

Kabbour, H., David, R., Pautrat, A., Koo, H. J., Whangbo, M. H., André, G. & Mentré, O. (2012). *Angew. Chem. Int. Ed.* **51**, 11745–11749.

Martin, N., Regnault, L. P. & Klimko, S. (2012). *J. Phys. Conf. Ser.* **340**, 012012-1–012012-9.

Moqine, A., Boukhari, A. & Darriet, J. (1993). *J. Solid State Chem.* **107**, 362–367.

Niesen, S. K., Heyer, O., Lorenz, T. & Valldor, M. (2011). *J. Magn. Magn. Mater.* **323**, 2575–2578.

Osterloh, D. & Müller-Buschbaum, H. (1994a). *Z. Naturforsch. Teil B*, **49**, 923–926.

Osterloh, D. & Müller-Buschbaum, H. (1994b). *Z. Anorg. Allg. Chem.* **620**, 651–654.

Rigaku (1998). *REQAB*. Rigaku Corporation, Tokyo, Japan.

Rigaku (2006). *CrystalClear*. Rigaku Corporation, Tokyo, Japan.

Rogado, N., Huang, Q., Lynn, J., Ramirez, A. P., Huse, D. & Cava, R. J. (2002). *Phys. Rev. B*, **65**, 144443-1–144443-7.

Shannon, R. D. (1976). *Acta Cryst.* A**32**, 751–767.

Sheldrick, G. M. (2015a). *Acta Cryst.* A**71**, 3–8.

Sheldrick, G. M. (2015b). *Acta Cryst.* C**71**, 3–8.

Uchiyama, Y., Sasago, Y., Tsukada, I., Uchinokura, K., Zheludev, A., Hayashi, T., Miura, N. & Böni, P. (1999). *Phys. Rev. Lett.* **83**, 632–635.

Ulutagay-Kartin, M., Hwu, S.-J. & Clayhold, J. A. (2003). *Inorg. Chem.* **42**, 2405–2409.

Velikodnyi, Y. A., Trunov, V. K., Zhuravlev, V. D. & Makarevich, L. G. (1982). *Sov. Phys. Crystallogr.* **27**, 226–229.

Vogt, R. & Müller-Buschbaum, H. (1990). *Z. Anorg. Allg. Chem.* **591**, 167–173.

Von Postel, M. & Müller-Buschbaum, H. (1992). *Z. Anorg. Allg. Chem.* **615**, 97–100.

Weil, M. (2016). *Cryst. Growth Des.* **16**, 908–921.

Weil, M. & Kremer, R. K. (2017). *J. Solid State Chem.* **245**, 115–126.

Westrip, S. P. (2010). *J. Appl. Cryst.* **43**, 920–925.

Wichmann, R. & Müller-Buschbaum, H. (1986a). *Z. Anorg. Allg. Chem.* **534**, 153–158.

Wichmann, R. & Müller-Buschbaum, Hk. (1986b). *Rev. Chim. Miner.* **23**, 1–7.

Yang, M., Zhang, S. Y., Guo, W. B. & He, Z. Z. (2016). *Solid State Sci.* **52**, 72–77.

Crystal structure of BaMn$_2$(AsO$_4$)$_2$ containing discrete [Mn$_4$O$_{18}$]$^{28-}$ units

Salvador Alcantar, Hollis R. Ledbetter and Kulugammana G. S. Ranmohotti

Computing details

Data collection: *CrystalClear* (Rigaku, 2006); cell refinement: *CrystalClear* (Rigaku, 2006); data reduction: *CrystalClear* (Rigaku, 2006); program(s) used to solve structure: SHELXT (Sheldrick, 2015*a*); program(s) used to refine structure: *SHELXL2014* (Sheldrick, 2015*b*); molecular graphics: *DIAMOND* (Brandenburg, 1999); software used to prepare material for publication: *publCIF* (Westrip, 2010).

Barium dimanganese(II) bis(arsenate)

Crystal data

BaMn$_2$(AsO$_4$)$_2$	$Z = 2$
$M_r = 525.06$	$F(000) = 472$
Triclinic, $P\bar{1}$	$D_x = 4.787$ Mg m^{-3}
$a = 5.7981$ (12) Å	Mo $K\alpha$ radiation, $\lambda = 0.71073$ Å
$b = 7.0938$ (14) Å	Cell parameters from 3100 reflections
$c = 9.817$ (2) Å	$\theta = 2.3$–25.2°
$\alpha = 109.75$ (3)°	$\mu = 17.78$ mm^{-1}
$\beta = 100.42$ (3)°	$T = 293$ K
$\gamma = 98.40$ (3)°	Column, light pink
$V = 364.26$ (15) Å^3	$0.20 \times 0.10 \times 0.06$ mm

Data collection

Rigaku AFC8S diffractometer	1330 independent reflections
Radiation source: fine-focus sealed tube	1254 reflections with $I > 2\sigma(I)$
φ and ω scans	$R_{int} = 0.035$
Absorption correction: multi-scan (*REQAB*; Rigaku, 1998)	$\theta_{max} = 25.5°$, $\theta_{min} = 2.3°$
	$h = -6 \rightarrow 7$
$T_{min} = 0.808$, $T_{max} = 1.000$	$k = -8 \rightarrow 8$
3149 measured reflections	$l = -11 \rightarrow 11$
	1 standard reflections every 1 reflections

Refinement

Refinement on F^2	Secondary atom site location: difference Fourier map
Least-squares matrix: full	
$R[F^2 > 2\sigma(F^2)] = 0.039$	$w = 1/[\sigma^2(F_o^2) + (0.0674P)^2 + 0.2802P]$ where $P = (F_o^2 + 2F_c^2)/3$
$wR(F^2) = 0.097$	
$S = 1.14$	$(\Delta/\sigma)_{max} = 0.001$
1330 reflections	$\Delta\rho_{max} = 3.25$ e Å^{-3}
119 parameters	$\Delta\rho_{min} = -2.93$ e Å^{-3}
0 restraints	Extinction correction: SHELXL2014 (Sheldrick, 2015a),
Primary atom site location: structure-invariant direct methods	Fc*=kFc[1+0.001xFc$^2\lambda^3$/sin(2θ)]$^{-1/4}$
	Extinction coefficient: 0.076 (3)

Special details

Geometry. All esds (except the esd in the dihedral angle between two l.s. planes) are estimated using the full covariance matrix. The cell esds are taken into account individually in the estimation of esds in distances, angles and torsion angles; correlations between esds in cell parameters are only used when they are defined by crystal symmetry. An approximate (isotropic) treatment of cell esds is used for estimating esds involving l.s. planes.

Fractional atomic coordinates and isotropic or equivalent isotropic displacement parameters (Å²)

	x	*y*	*z*	U_{iso}*/U_{eq}
Ba1	0.24355 (7)	0.79849 (6)	0.05371 (4)	0.0100 (2)
Mn1	0.36901 (17)	1.15237 (15)	0.44407 (11)	0.0091 (3)
Mn2	0.00727 (18)	0.59526 (15)	0.35472 (12)	0.0105 (3)
As1	−0.15775 (11)	1.02502 (10)	0.30239 (7)	0.0061 (3)
As2	0.40017 (11)	0.42782 (10)	0.24010 (7)	0.0062 (3)
O1	−0.3934 (8)	0.9502 (7)	0.3669 (5)	0.0092 (10)
O2	0.3546 (8)	0.1879 (7)	0.2382 (5)	0.0124 (10)
O3	0.0571 (8)	0.8910 (7)	0.3296 (5)	0.0105 (10)
O4	0.3801 (8)	0.5917 (7)	0.4075 (5)	0.0099 (10)
O5	−0.0125 (8)	1.2729 (7)	0.4122 (5)	0.0125 (10)
O6	−0.2437 (9)	0.9808 (7)	0.1213 (5)	0.0139 (11)
O7	0.1684 (8)	0.4587 (7)	0.1276 (6)	0.0133 (11)
O8	0.6676 (8)	0.4888 (7)	0.2047 (5)	0.0127 (10)

Atomic displacement parameters (Å²)

	U^{11}	U^{22}	U^{33}	U^{12}	U^{13}	U^{23}
Ba1	0.0116 (3)	0.0073 (3)	0.0072 (3)	−0.00194 (18)	0.00103 (18)	0.0003 (2)
Mn1	0.0061 (5)	0.0097 (5)	0.0073 (5)	−0.0021 (4)	0.0006 (4)	0.0000 (4)
Mn2	0.0053 (5)	0.0125 (6)	0.0087 (6)	0.0006 (4)	0.0003 (4)	−0.0009 (4)
As1	0.0043 (4)	0.0072 (4)	0.0043 (4)	−0.0005 (3)	0.0007 (3)	−0.0001 (3)
As2	0.0036 (4)	0.0060 (4)	0.0069 (4)	−0.0002 (3)	0.0007 (3)	0.0007 (3)
O1	0.006 (2)	0.011 (2)	0.010 (2)	0.0021 (17)	0.0015 (17)	0.0034 (19)
O2	0.017 (2)	0.006 (2)	0.012 (3)	0.0009 (18)	0.0022 (19)	0.0023 (19)
O3	0.006 (2)	0.009 (2)	0.016 (3)	0.0021 (17)	0.0009 (18)	0.005 (2)
O4	0.009 (2)	0.009 (2)	0.008 (2)	0.0015 (18)	0.0040 (17)	−0.0008 (18)
O5	0.013 (2)	0.013 (2)	0.006 (2)	−0.0032 (18)	0.0037 (18)	−0.001 (2)
O6	0.017 (3)	0.018 (3)	0.004 (2)	0.002 (2)	−0.0009 (19)	0.004 (2)
O7	0.008 (2)	0.013 (2)	0.016 (3)	−0.0008 (18)	−0.0042 (19)	0.007 (2)
O8	0.006 (2)	0.018 (2)	0.011 (2)	−0.0018 (18)	0.0055 (18)	0.002 (2)

Geometric parameters (Å, º)

Ba1—O2[i]	2.647 (4)	Mn2—O8[viii]	2.094 (5)
Ba1—O7[ii]	2.682 (5)	Mn2—O4	2.136 (5)
Ba1—O6[iii]	2.687 (5)	Mn2—O5[vii]	2.152 (5)
Ba1—O7	2.741 (5)	Mn2—O3	2.178 (5)
Ba1—O8[iv]	2.853 (5)	Mn2—O7	2.518 (5)
Ba1—O6[v]	2.921 (5)	Mn2—O5[ix]	2.526 (5)

Ba1—O3	3.000 (5)	As1—O6	1.663 (5)
Ba1—O1^{v}	3.131 (5)	As1—O1	1.697 (5)
Mn1—O4^{vi}	2.052 (5)	As1—O5	1.709 (5)
Mn1—O2^{i}	2.108 (5)	As1—O3	1.710 (4)
Mn1—O1^{v}	2.179 (4)	As2—O7	1.669 (5)
Mn1—O1^{vii}	2.200 (5)	As2—O2	1.677 (5)
Mn1—O3	2.202 (5)	As2—O8	1.677 (4)
Mn1—O5	2.491 (5)	As2—O4	1.698 (5)
Mn1—Mn1^{vi}	3.185 (2)		
O2^{i}—Ba1—O7^{ii}	133.63 (15)	O8^{viii}—Mn2—O5^{ix}	94.05 (18)
O2^{i}—Ba1—O6^{iii}	74.41 (15)	O4—Mn2—O5^{ix}	79.10 (17)
O7^{ii}—Ba1—O6^{iii}	90.91 (15)	O5^{vii}—Mn2—O5^{ix}	81.45 (17)
O2^{i}—Ba1—O7	127.00 (15)	O3—Mn2—O5^{ix}	173.25 (17)
O7^{ii}—Ba1—O7	71.27 (16)	O7—Mn2—O5^{ix}	94.82 (16)
O6^{iii}—Ba1—O7	158.19 (14)	O6—As1—O1	111.1 (2)
O2^{i}—Ba1—O8^{iv}	144.78 (15)	O6—As1—O5	114.6 (2)
O7^{ii}—Ba1—O8^{iv}	69.26 (14)	O1—As1—O5	110.1 (2)
O6^{iii}—Ba1—O8^{iv}	79.72 (15)	O6—As1—O3	109.1 (2)
O7—Ba1—O8^{iv}	82.17 (15)	O1—As1—O3	109.0 (2)
O2^{i}—Ba1—O6^{v}	67.93 (15)	O5—As1—O3	102.5 (2)
O7^{ii}—Ba1—O6^{v}	152.74 (15)	O7—As2—O2	111.2 (2)
O6^{iii}—Ba1—O6^{v}	78.74 (16)	O7—As2—O8	114.4 (3)
O7—Ba1—O6^{v}	111.37 (14)	O2—As2—O8	109.7 (2)
O8^{iv}—Ba1—O6^{v}	84.02 (14)	O7—As2—O4	99.8 (2)
O2^{i}—Ba1—O3	63.79 (14)	O2—As2—O4	109.1 (2)
O7^{ii}—Ba1—O3	94.34 (15)	O8—As2—O4	112.2 (2)
O6^{iii}—Ba1—O3	126.26 (14)	As1—O1—Mn1^{viii}	121.9 (2)
O7—Ba1—O3	69.23 (14)	As1—O1—Mn1^{vii}	125.5 (2)
O8^{iv}—Ba1—O3	150.59 (13)	Mn1^{viii}—O1—Mn1^{vii}	93.34 (18)
O6^{v}—Ba1—O3	112.17 (13)	As1—O1—Ba1^{viii}	93.03 (18)
O2^{i}—Ba1—O1^{v}	58.18 (14)	Mn1^{viii}—O1—Ba1^{viii}	85.45 (14)
O7^{ii}—Ba1—O1^{v}	146.18 (14)	Mn1^{vii}—O1—Ba1^{viii}	133.22 (19)
O6^{iii}—Ba1—O1^{v}	121.73 (13)	As2—O2—Mn1^{ix}	117.6 (2)
O7—Ba1—O1^{v}	78.33 (13)	As2—O2—Ba1^{ix}	141.9 (3)
O8^{iv}—Ba1—O1^{v}	121.31 (13)	Mn1^{ix}—O2—Ba1^{ix}	100.46 (18)
O6^{v}—Ba1—O1^{v}	54.34 (13)	As1—O3—Mn2	127.5 (2)
O3—Ba1—O1^{v}	60.47 (12)	As1—O3—Mn1	98.5 (2)
O4^{vi}—Mn1—O2^{i}	102.96 (19)	Mn2—O3—Mn1	127.0 (2)
O4^{vi}—Mn1—O1^{v}	99.75 (17)	As1—O3—Ba1	104.3 (2)
O2^{i}—Mn1—O1^{v}	82.98 (19)	Mn2—O3—Ba1	101.98 (16)
O4^{vi}—Mn1—O1^{vii}	84.93 (19)	Mn1—O3—Ba1	88.38 (16)
O2^{i}—Mn1—O1^{vii}	167.89 (17)	As2—O4—Mn1^{vi}	127.8 (3)
O1^{v}—Mn1—O1^{vii}	86.66 (18)	As2—O4—Mn2	99.8 (2)
O4^{vi}—Mn1—O3	166.2 (2)	Mn1^{vi}—O4—Mn2	121.3 (2)
O2^{i}—Mn1—O3	88.15 (19)	As1—O5—Mn2^{vii}	122.2 (3)
O1^{v}—Mn1—O3	89.68 (17)	As1—O5—Mn1	88.39 (19)
O1^{vii}—Mn1—O3	85.54 (18)	Mn2^{vii}—O5—Mn1	97.19 (19)

O4^{vi}—Mn1—O5	104.50 (16)	As1—O5—Mn2ⁱ	129.8 (3)
O2ⁱ—Mn1—O5	79.89 (17)	Mn2^{vii}—O5—Mn2ⁱ	98.55 (17)
O1^v—Mn1—O5	152.85 (16)	Mn1—O5—Mn2ⁱ	116.29 (18)
O1^{vii}—Mn1—O5	107.30 (17)	As1—O6—Ba1ⁱⁱⁱ	137.3 (3)
O3—Mn1—O5	68.96 (16)	As1—O6—Ba1^{viii}	101.6 (2)
O8^{viii}—Mn2—O4	150.46 (18)	Ba1ⁱⁱⁱ—O6—Ba1^{viii}	101.26 (16)
O8^{viii}—Mn2—O5^{vii}	116.23 (18)	As2—O7—Mn2	87.0 (2)
O4—Mn2—O5^{vii}	91.36 (18)	As2—O7—Ba1ⁱⁱ	132.7 (2)
O8^{viii}—Mn2—O3	92.31 (19)	Mn2—O7—Ba1ⁱⁱ	96.77 (16)
O4—Mn2—O3	96.40 (18)	As2—O7—Ba1	116.9 (2)
O5^{vii}—Mn2—O3	93.72 (19)	Mn2—O7—Ba1	100.85 (16)
O8^{viii}—Mn2—O7	85.61 (17)	Ba1ⁱⁱ—O7—Ba1	108.73 (16)
O4—Mn2—O7	66.64 (17)	As2—O8—Mn2^v	127.9 (3)
O5^{vii}—Mn2—O7	157.97 (16)	As2—O8—Ba1^{iv}	116.1 (2)
O3—Mn2—O7	87.90 (17)	Mn2^v—O8—Ba1^{iv}	102.60 (17)

Symmetry codes: (i) x, $y+1$, z; (ii) $-x$, $-y+1$, $-z$; (iii) $-x$, $-y+2$, $-z$; (iv) $-x+1$, $-y+1$, $-z$; (v) $x+1$, y, z; (vi) $-x+1$, $-y+2$, $-z+1$; (vii) $-x$, $-y+2$, $-z+1$; (viii) $x-1$, y, z; (ix) x, $y-1$, z.